Supplementary information

for

Valley polarization by spin injection in a light-emitting van der Waals heterojunction

Oriol Lopez Sanchez[1,2], Dmitry Ovchinnikov[1,2], Shikhar Misra[3], Adrien Allain[1,2], Andras Kis[1,2*]

[1]*Electrical Engineering Institute, École Polytechnique Fédérale de Lausanne (EPFL), CH-1015 Lausanne, Switzerland*
[1]*Instutute of Materials Science and Engineering, École Polytechnique Fédérale de Lausanne (EPFL), CH-1015 Lausanne, Switzerland*
[2]*Department of Materials Science and Engineering, Indian Institute of Technology (IIT), Kanpur 208016, India*

**Correspondence should be addressed to: Andras Kis, andras.kis@epfl.ch*

1. Band profile of the device

We present on Supplementary Figure 1 the band profile of the MoS_2/WSe_2 heterojunction together with the contacts for electron and hole injection.

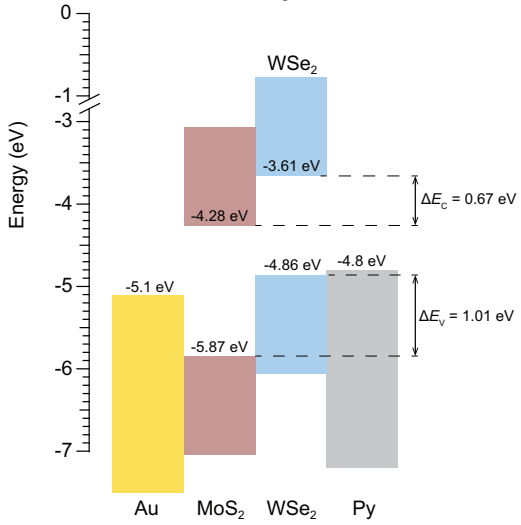

Supplementary Figure 1. Band profile of the WSe_2/MoS_2 heterojunction LED in the lateral direction.

Band alignment for the MoS_2/WSe_2 heterostructure was calculated by Kang et al.[1], while the work function of permalloy is 4.8 eV (ref. 2).

2. Electroluminescence spectra for different excitation currents

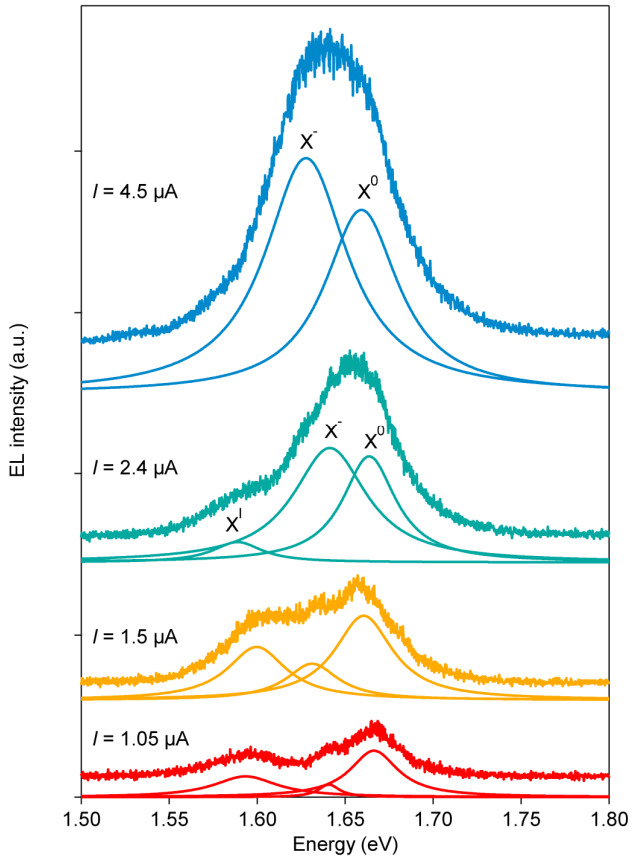

Supplementary Figure 2. Evolution of the electroluminescence spectra. As the current is increased electroluminescence from the negatively charged X^- exciton begins to dominate.

3. Electroluminescence map for the device with ferromagnetic contacts

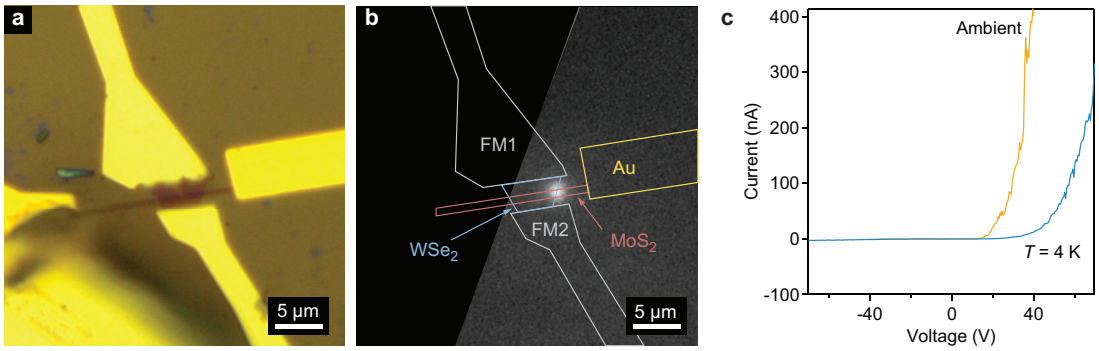

Supplementary Figure 3. **a,** Optical image of the device based on a monolayer WSe_2/monolayer MoS_2 heterojunction contacted using a ferromagnetic electrode and presented in the main text. **b,** intensity map showing the electroluminescent emission with superimposed outline of the most important device components. **c,** current-voltage characteristic of this device, showing rectification. The curve was acquired at the end of the characterization run and shows current levels lower than on Figure 1 in the main manuscript.

Supplementary Figure 3 shows an optical image of the device with ferromagnetic electrodes presented in the main text, together with an electroluminescence intensity map. The light emission is most intense at the edge of the heterojunction.

4. Curve fitting

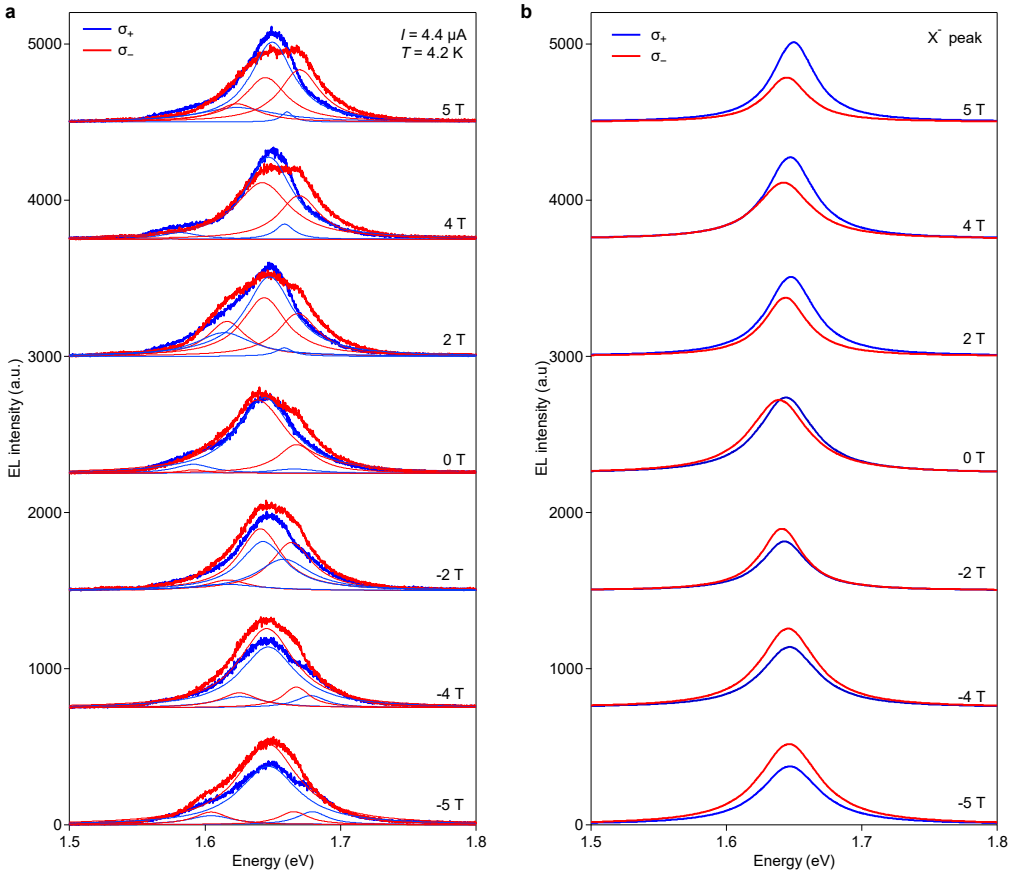

Supplementary Figure 4. Fitting of electroluminescence spectra. a, Electroluminescence data fitted with multiple Lorentzian peaks. b, Evolution of the X^- peak extracted from the fits for different polarizations, as a function of the magnetic field.

5. Control device with non-magnetic electrodes

In order to verify spin injection in WSe_2/MoS_2 heterostructures with ferromagnetic contacts, we fabricate a second set of devices in which the magnetic permalloy electrode has been substituted by a palladium/gold (Pd/Au) electrode, Supplementary Figure 5, while the rest of the device fabrication and characterization procedure was left unchanged.

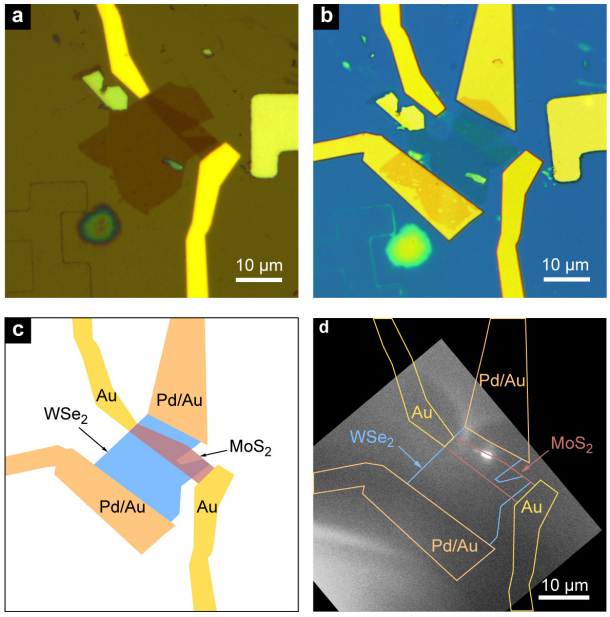

Supplementary Figure 5. Electroluminescent device based on a WSe_2/MoS_2 heterojunction with non-magnetic electrodes. **a,** optical image after the deposition of the first set of electrodes. **b,** optical image of the final device with Pd/Au electrodes contacting WSe_2 and after encapsulation with HfO_2. **c,** outline of the device. **d,** intensity map showing the electroluminescent emission with superimposed outline of the most important device components.

Supplementary Figure 5d shows a superposition of the electroluminescence map on the same device area as in parts a-c. Only the top Au and Pd/Au electrodes were biased. Light emission is localized at center of the edge of WSe_2/MoS_2 heterojunction closest to the hole injecting electrode. Electroluminescence spectra from this device with non-magnetic contacts, for different values of the external magnetic field, are shown on Supplementary Figure 6.

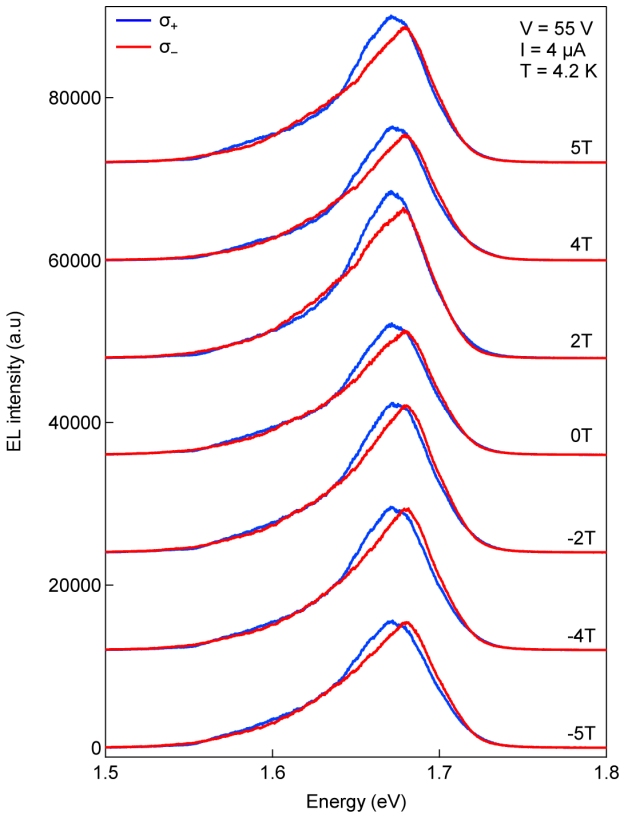

Supplementary Figure 6. Electroluminescence spectra from a device with non-magnetic contacts acquired for different values of magnetic fields, acquired for σ_+ and σ_- polarizations.

The change in the degree of circular polarisation as a function of external magnetic field is on the order of ~0.5%/T and is attributed to valley polarisation in the WSe_2 due to the magnetic field[3,4]. By subtracting this contribution from the total response of the device with the ferromagnetic electrode, we can extract the contribution to circular polarisation due to spin polarisation of charge carriers. Moreover, we can see from Supplementary Figure 7b that the polarization stops significantly increasing above ± 2T, indicating the presence of saturation in the magnetisation of the permalloy electrode.

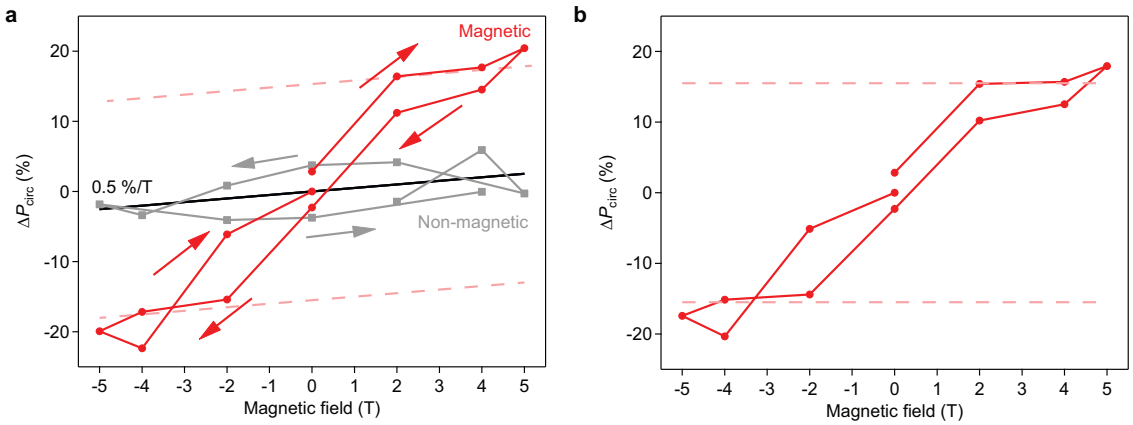

Supplementary Figure 7. **a,** Dependence of the relative difference in degree of circular polarization of the X^- resonance as a function of the external magnetic field for a device with a magnetic (PY) electrode and for a control device with non-magnetic electrodes. Dashed red lines run parallel to the ~0.5 %/T contribution to valley polarization in WSe_2 due to the applied magnetic field. **b,** Dependence of the relative difference in degree of circular polarization of the X− resonance as a function of external magnetic field for a device with a magnetic (PY) electrode after the subtraction of the intrinsic circular dichroism due to the external magnetic field.

REFERENCES

(1) Kang, J.; Tongay, S.; Zhou, J.; Li, J.; Wu, J. Band Offsets and Heterostructures of Two-Dimensional Semiconductors. *Appl. Phys. Lett.* **2013**, *102*, 12111.

(2) Wang, W.; Liu, Y.; Tang, L.; Jin, Y.; Zhao, T.; Xiu, F. Controllable Schottky Barriers between MoS_2 and Permalloy. *Sci. Rep.* **2014**, *4*.

(3) MacNeill, D.; Heikes, C.; Mak, K. F.; Anderson, Z.; Kormányos, A.; Zólyomi, V.; Park, J.; Ralph, D. C. Breaking of Valley Degeneracy by Magnetic Field in Monolayer $MoSe_2$. *Phys. Rev. Lett.* **2015**, *114*, 37401.

(4) Srivastava, A.; Sidler, M.; Allain, A. V.; Lembke, D. S.; Kis, A.; Imamoğlu, A. Valley Zeeman Effect in Elementary Optical Excitations of Monolayer WSe_2. *Nat. Phys.* **2015**, *11*, 141–147.